A novel formalism for calculating positron annihilation characteristics

1991 J. Phys.: Condens. Matter 3 163

(http://iopscience.iop.org/0953-8984/3/2/003)

J. Phys.: Condens. Matter 3 (1991) 163–175. Printed in the UK

A novel formalism for calculating positron annihilation characteristics

Lou Yongming†‡, R M Nieminen§ and B Johansson†
† Condensed Matter Theory Group, Physics Department, Uppsala University, Box 530, S-75121 Uppsala, Sweden
‡ Physics Department, Tsinghua University, Beijing, China
§ Laboratory of Physics, Helsinki University of Technology, 02150 Espoo, Finland

Received 12 February 1990, in final form 11 October 1990

Abstract. We propose a novel formalism to calculate the positron annihilation characteristics in solids in which the positron–electron product (PEP) wavefunction is obtained directly from a wave equation. From this PEP equation it is easy to see that the most structure-dependent term, the Coulomb potential, present in the individual electron and positron wave equations is cancelled exactly. The remaining potential is a considerably smoother and weaker function than the Coulomb potential. In a qualitative analysis, one can then easily explain some typical but apparently paradoxical features in earlier treatments. As an illustration of the PEP formalism we have calculated the bulk angular correlation distribution of a positron annihilating in Al metal. Within the new formalism the effect of the crystalline potential (symmetry) and of the many-body interaction on the angular correlation distribution can be calculated in a phenomenological way. The results are in good agreement with experiments, even as regards the finer details, and compare well with the conventional formalism. The advantages and shortcomings of the new formalism are discussed.

1. Introduction

In recent years, both the theory and the experiment of the angular distribution of electron–positron annihilation (i.e. angular correlation of annihilation radiation, ACAR) have made considerable progress [1]. The higher precision achieved in the experiments makes it possible to compare them with detailed theoretical calculations. It is a well known fact that the positron disturbs the electronic structure near the region where the annihilation takes place. However, without a proper correction due to the positron–electron many-body enhancement, this effect is difficult to treat properly in the traditional way to calculate the ACAR distribution, in which the electron and positron wavefunctions are solved separately. Owing to the small mass of the positron and the extreme imbalance between the number of electrons (10^{23}) and the single positron, the effective density of the delocalized positron will be nearly zero, which gives rise to the fact that in the theoretical treatment the electronic structure is left unchanged even in the presence of the positron. This difficulty will to some extent be removed by a proper treatment of the many-body effect. In situations where the positron is localized in space when the annihilation takes place, the treatment of the deformation of the local electronic structure due to the positron can be studied more easily, and good agreement

0953-8984/91/020163 + 13 $03.50

between the theoretical and experimental results has been obtained [2–4]. In the case of a delocalized positron, the self-consistent scheme [5] for the whole system containing all electrons and one positron suffers from the inability to deal with an infinitely small density of the delocalized positron. Thus the electronic structure is kept unperturbed even in the presence of the positron and the treatment of the many-electron and one-positron system is, in fact, broken down into a separate calculation of the positron and a self-consistent treatment of the electrons.

In order to include the effect of the positron–electron many-body interaction, a lot of effort has been expended over the years through the treatment of the so-called enhancement or de-enhancement factor for the jellium model [6–9]. It has become well established how to incorporate the many-body enhancement or de-enhancement factor into the calculation of the angular correlation distribution. Nevertheless, owing to the various approximations used in calculating the electron and positron wavefunctions and the difficulty of calculating the enhancement or de-enhancement in a band-structure calculation, it sometimes seems difficult to decide upon which enhancement factor is more appropriate than others [10]. In some cases this is done in a phenomenological way, i.e. adjusting the enhancement factor with several parameters to fit the experiment [10]. Therefore calculations that treat the electron and positron wavefunctions separately sometimes give rise to difficulties in the understanding of the experimental results. An example is the case of the bulk ACAR for a simple metal. The experimental long-slit ACAR of an Al single crystal is well represented by a free-electron parabola [11, 12], except for some extended bulges, which do not fit the parabolic form. These have been attributed to electron–positron many-body effects [6, 7]. The earlier success in explaining the ACAR results for simple metals suggested that the positron wavefunction is nearly constant and that the electron wavefunctions are essentially free plane waves. It is also a well known fact that the energy band structure of the simple metals can be obtained from electron pseudo-wavefunctions. The pseudo-wavefunction is similar to a free plane wave and is only weakly perturbed by the crystal potential. However, the true electron wavefunction contains strong oscilations in the atomic core regions. In addition the true positron wavefunction is also affected by a strong crystal potential in the core region. Thus there is an apparent paradox: the true electron and positron wavefunctions would seem to predict much more structure in the ACAR distribution than is found experimentally.

The second observation is that the ACAR for a positron localized at a defect in one or more dimensions so far as always been found to be narrower than that for the bulk positron state. For example, ACAR from a positron in a vacancy or a void is narrower than that from the bulk [3, 4, 13, 14]. In the earlier treatments, which were based on the jellium model [13, 14] and supercell model [3, 4], the narrowing has been explained for the vacancy and void cases. Recently, a surface potential model [15, 16] has been used to explain the unexpected, nearly isotropic and narrowed experimental ACAR for the Al and Cu surfaces [17, 18]. In the case of a positron in an atomic bubble in a metal, the experimental ACAR is again found to be narrower than for the bulk [19]. These narrower ACAR results could be well explained by detailed calculations based on the traditional formalism. However, it is not easy to formulate a simple physical picture for the narrowing effect, especially not its systematics.

In this paper we propose a new, simple formalism to calculate the positron annihilation characteristics such as the angular correlation distribution and the positron lifetime. Instead of solving the electron and positron wavefunctions separately, we directly calculate the positron–electron product wavefunction. In this formalism, the

electron–positron interaction and the many-body interaction are included in the calculation of the positron–electron product wavefunction through a phenomenological total effective potential. We show that one thereby can easily and systematically explain the qualitative features of the annihilation characteristics. As a prototype we use Al and calculate the bulk angular correlation distribution. We find that we can account for most of the small extended bulges found experimentally by means of a phenomenological total effective potential for the positron–electron product wavefunction that includes the effective electron–electron and electron–positron many-body interaction.

2. Theoretical formalism

Usually positron annihilation characteristics are calculated by means of a formalism in which the electron and positron wavefunctions are solved separately [3, 5, 11], i.e. the electron wavefunctions ψ_i in a crystal are obtained from the Kohn–Sham equations (with $\hbar = e^2/2 = 2m = 1$)

$$-\nabla^2\psi_i + V_e\psi_i = E_i\psi_i \tag{1}$$

where $V_e = V_C + V_{xc} + V_{e,corr}[n(\boldsymbol{r}), n^+(\boldsymbol{r})]$. Here V_C, V_{xc} and $V_{e,corr}$ are the Coulomb potential and exchange–correlation potential and the electron–positron correlation potential, respectively; E_i, $n(\boldsymbol{r})$ and $n^+(\boldsymbol{r})$ are the energy eigenvalue for the electron, the electron density and the positron density, respectively. In the case of a fully delocalized positron, n^+ is equal to $1/V$ where V is the volume of the experimental sample. Owing to the infinitely small value of the positron density, $V_{e,corr}$ will be equal to zero or a constant, which can be omitted as has been done in almost every calculation of the bulk ACAR. For the same reason, the contribution to the Coulomb potential from the positron is also omitted in the perfect crystal. Thus the electronic structure will be kept unchanged even in the presence of a positron. This difficulty can to a large extent be avoided in the case of a defect crystal, in which the positron density in the defect may be comparable to the electron density, such as in a vacancy or divacancy [3, 4].

The corresponding positron wavefunction ψ_+ obeys the equation

$$-\nabla^2\psi_+ + V_+\psi_+ = E_+\psi_+ \tag{2}$$

where $V_+ = -V_C + V_{corr}$. Here V_{corr} is the positron–electron correlation potential and E_+ is the positron energy eigenvalue. The momentum distribution $\rho^{2\gamma}(\boldsymbol{p})$ of the annihilating positron–electron pair is calculated within the independent-particle model (IPM) [11]

$$\rho^{2\gamma}(\boldsymbol{p}) = \text{const} \sum_i^{occ} \left| \int d\boldsymbol{r} \exp(-i\boldsymbol{p}\cdot\boldsymbol{r})\psi_+(\boldsymbol{r})\psi_i(\boldsymbol{r}) \right|^2 \tag{3}$$

where $\boldsymbol{p}$ is the total momentum of 2γ photons, and the summation is over all occupied electron states.

The various approximations used in the traditional way to treat equations (1) and (2) can give rise to difficulties in the Fourier transformation of equation (3). In fact, these might even produce spurious oscillations in $\rho^{2\gamma}(\boldsymbol{p})$.

We propose a novel formalism to calculate the positron annihilation characteristics. Rather than solving equations (1) and (2) individually and with a very high precision, we obtain the positron–electron product (PEP) wavefunction $\psi_i\psi_+$ directly. From

equations (1) and (2), one easily sees that the PEP wavefunction obeys the following equation:

$$-\nabla^2(\psi_i\psi_+) + U^*(\psi_i\psi_+) = (E_+ + E_i)(\psi_i\psi_+)$$
$$U^* = 2(\nabla\psi_i \cdot \nabla\psi_+)/(\psi_i\psi_+) + V_{xc} + V_{corr} + V_{e,corr} + V_u. \tag{4}$$

Above, U^* plays the role of a total effective potential for the positron–electron product wavefunction. The potential V_u consists of two parts. One part comes from the very small difference between the Coulomb potentials for the electron and for the positron, which so far has been neglected in ACAR calculations [20]. The other part is the difference between the true and the employed interaction [20]. From equation (4) we find that the strong and most structure-dependent term V_C is cancelled exactly except for the very small difference between the Coulomb potentials for the electron and for the positron [20]. The remaining terms V_{xc}, V_{corr}, V_u and $V_{e,corr}$ are smooth functions. The term $\nabla\psi_i \cdot \nabla\psi_+$ can be estimated from the calculation of Stroud *et al* [21], in which electron and positron pseudo-wavefunctions similar to the pseudo-wavefunctions in [22] were used. From the results in [22] for Al, we know that more than 90% of the positron wavefunction is a constant and therefore the gradient term will not have strong oscillations outside of the core region in simple metals. From a comparison between the ACAR of the positron annihilation and the recent high-resolution Compton profiles for Al and Si [23, 24], one can clearly see that the high-momentum part of the Compton profiles is much more pronounced than the corresponding angular correlation curve for the positron annihilation. This suggests that the effective potential in the PEP equation is weaker than the effective potential for the electron. This is consistent with our expectations based on the cancellation of the strong Coulomb potential. It is also known that the electronic structure of the valence and conduction bands in simple metals and some semiconductors is well represented by pseudopotential calculations. Thus the total effective potential U^* is weaker than the electron pseudopotential or at least of the same order. Taking advantage of the similarity between the PEP equation in momentum space and the pseudopotential formalism for the electron, we can calculate the positron–electron product wavefunction directly from the momentum space through a few phenomenological potential parameters. In this way, we can avoid the difficulty that, at present, we do not know the exact form of the electron–electron and electron–positron many-body interaction. The drawbacks of this scheme are the same as for the empirical pseudopotential formalism for the electrons, such as: detailed information of the many-body interaction is lost in the potential parameters and at the present stage the potential parameters can only be obtained from a fitting to experiments. Nevertheless, this scheme has the important advantage that the electron–positron interaction can be dealt with in the calculation of the PEP, which has not been included in the traditional way to calculate the electron wavefunction owing to the nearly zero density for a delocalized positron. Having obtained the PEP wavefunction $\psi_i\psi_+$, one can use equation (4) to calculate the momentum distribution $\rho^{2\gamma}(p)$. The positron lifetime τ (i.e. the inverse of the annihilation rate λ) is, within the local density approximation [25],

$$1/\tau = \lambda = \int_{-\infty}^{\infty} dr\, \Gamma\, |\psi_+(r)|^2\, n(r) = \int_{-\infty}^{\infty} dr\, \Gamma \sum_{i}^{occ} |\psi_+(r)\psi_i(r)|^2 \tag{5}$$

where $n(r)$ is the electron density. The enhancement factor Γ, which will be discussed in detail elsewhere, can be approximated as [26]

$$\Gamma = (2/n_0 + 134) \times 10^9\ s^{-1}. \tag{6}$$

Thus Γ depends only on the average electron density n_0.

In a qualitative analysis, one can now easily resolve the mentioned apparent paradoxes. Although, individually, both the electron and the positron wavefunctions are strongly affected by the crystal potential, the positron–electron product wavefunction is much less influenced. Therefore, in the case of a bulk positron annihilation process for a simple metal, one obtains an angular correlation distribution that is similar to the free-electron behaviour. In the case of a localized positron, the product form will also lead to a narrower angular distribution than for a delocalized case.

The potential U^* is in fact likely to be even weaker than the electron pseudopotential. This can be understood qualitatively from the fact that the positron–electron pair behaves like a neutral quasiparticle. It is the weakness of U^* that gives rise to the nearly parabolic shape with some extended bulges (also observed experimentally) and at the same time does not produce the erroneous extra structure in the angular correlation distribution sometimes found from traditional calculations. This will be discussed further in section 3.

As one can see from equations (3) and (5), the positron annihilation characteristics depend only on the Fourier transform of the product $\psi_i\psi_+$. Therefore it is natural to solve the PEP equation in reciprocal space. In the following we denote

$$\Psi_{\mathrm{ep},i}(r) = \psi_i(r)\psi_+(r). \tag{7}$$

In reciprocal space $\Psi_{\mathrm{ep},k}$ and the total effective potential U^* for the positron–electron product wavefunction $\Psi_{\mathrm{ep},k}$ can be expanded as

$$\Psi_{\mathrm{ep},k}(r) = \sum_{G}^{\mathrm{all}} C_{-G}(k)\exp[\mathrm{i}(k-G)\cdot r]$$

$$U^*(r) = \sum_{G}^{\mathrm{all}} U_G \exp(\mathrm{i}G\cdot r) \tag{8}$$

$$U_G = \frac{1}{v}\int_{\mathrm{cell}} \mathrm{d}r \exp(-\mathrm{i}G\cdot r)U^*(r)$$

where k is the real crystal momentum in the extended zone scheme and v is the volume of the primitive cell. The sum in equation (8) is over all reciprocal lattice vectors. The coefficients $C_{-G}(k)$ and the energy E_k, which is equal to the sum of E_+ and E_i, are determined by the following set of equations:

$$[(k-G)^2 - E]C_{-G}(k) + \sum_{G'}^{\mathrm{all}} U_{G'-G}C_{-G'}(k) = 0. \tag{9}$$

Here we should emphasize that so far no additional approximations have been introduced in the PEP formalism. All approximations used up to equation (9), such as local-density approximation (LDA) and independent-particle approximation (IPA), are used in the traditional formalism and most of the electron energy band calculation formalism. All the terms of U^* including the gradient product term in equation (4) are transformed into U_G through equation (8) without any further approximation. In principle there are no constraints on any of the terms contributing to U^*. The only practical constraint is the limitation of the computer resources, which may appear when U^* is a strong potential because then a large number of reciprocal lattice vectors are needed in the calculation.

The square of the Fourier transform of $\Psi_{ep,k}$ is defined as $\Phi(p)$, where

$$\Phi(p) = \left| \int dr \exp(-ip \cdot r)\Psi_{ep,k}(r) \right|^2 = \left| \sum_G^{all} C_{-G}(k)\delta(k - p - G) \right|^2$$

$$= \sum_G^{all} |C_{-G}(k)|^2 \delta(k - p - G). \tag{10}$$

Before calculating the ACAR, we would like to discuss the normalization constant. It is known that the Schrödinger equation itself does not give the normalization constant of the wavefunction. Instead the normalization constant is imposed by the famous probability interpretation. In the present phenomenological PEP formalism, one also needs an assumption about the normalization constant of the PEP. As discussed above, it is plausible that for a material with only s and p electrons in the valence and conduction bands, such as simple metals and some semiconductors, the normalization constant will only be weakly dependent on the state of PEP. We assume that, for a crystal with only s and p electrons in its valence and conduction bands, the normalization constant $C_{norm}(E_k)$ for $\Psi_{ep,k}$ is only weakly dependent on the total energy corresponding to $\Psi_{ep,k}$ and can be approximately given by

$$C_{norm}(E_k) = C_{norm}(0)[1 + \alpha g(E_k)] \tag{11}$$

where α is a small constant that can be determined from experiment and $g(E_k)$ is a smooth function of E_k. The normalization constant might be approximately determined by a separate conventional calculation, assuming that the normalization constant of the positron–electron product wavefunction is unchanged from the conventional formalism to the PEP formalism. This will be discussed further elsewhere. At present the validity of the assumption can only be judged from the comparison between the calculated results and experiments. From our present results for Al and our ongoing work on Si [27], this assumption is found to be reasonable. In our calculations we therefore have simplified even further and used $\alpha = 0$ and removed $C_{norm}(0)$ from the ACAR calculation.

Then the angular correlation distribution $\rho^{2\gamma}(p)$ can be obtained as

$$\rho^{2\gamma}(p) = \sum_k^{all} f(E_k) \sum_G^{all} |C_{-G}(k)|^2 \delta(k - p - G) \tag{12}$$

$$f(E_k) = 1/\{\exp[(E_k - \mu)/k_B T] + 1\} \tag{13}$$

where $f(E_k)$ is the Fermi–Dirac distribution and μ the chemical potential. The order of summation in equation (12) can be interchanged to obtain

$$\rho^{2\gamma}(p) = \sum_G^{all} f(E_{p+G}) |C_{-G}(p + G)|^2. \tag{14}$$

The 2D angular correlation $I(p_x, p_y)$ is given by

$$I(p_x, p_y) = \int \rho^{2\gamma}(p)\, dp_z \tag{15}$$

and the 1D distributions $I(p_x)$ and $I(p_y)$ are

$$I(p_x) = \int I(p_x, p_y)\, dp_y \tag{16}$$

$$I(p_y) = \int I(p_x, p_y)\, dp_x \tag{17}$$

respectively.

We now discuss the calculated $\rho^{2\gamma}(\boldsymbol{p})$ for three cases, i.e. (i) $U^* = 0$, (ii) U^* is weak and (iii) U^* is not weak. For the case (i) $U^* = 0$ and $T = 0$ K, then

$$f(E_{p+G}) = \theta(E_F - E_{p+G}) \tag{18}$$

where E_F is the Fermi energy and θ the usual step function, and we immediately obtain

$$\rho^{2\gamma}(\boldsymbol{p}) = \theta(E_F - E_{p+G}) \tag{19}$$

and the 2D angular correlation $I_0(p_x, p_y)$ simplifies to

$$I_0(p_x, p_y) = 2(E_F - p_x^2 - p_y^2)^{1/2}. \tag{20}$$

The 1D angular correlation distribution $I_0(p_x)$ is then of the well known parabolic form

$$I_0(p_x) = \pi(E_F - p_x^2). \tag{21}$$

For non-zero temperatures, we use the Fermi–Dirac distribution for $\theta(E_F - E_{P+G})$ in equation (19) but we also have to consider other important temperature effects as well, such as the effective mass of the positron and the thermal expansion of the lattice constant a. The metals that can be relatively well described by this approximation include the alkalis, alkaline earths and aluminium [11, 28, 29]. Except for the small extended bulges, equation (21) accounts well for the experimental data.

In the case (ii), i.e. U^* weak, the rapid convergence of the sum in equation (14) means that it is only necessary to take into account the shortest reciprocal lattice vectors. For example, in FCC aluminium crystal, one [0, 0, 0], eight $\{\pm 1, \pm 1, \pm 1\}$ vectors (all permutations of signs) and six $\{\pm 2, 0, 0\}$ vectors (all permutations) are needed. Thus only four potential parameters are required, i.e. U_{111}, U_{002}, U_{220} and U_{311}, and we will set $U_{311} = U_{222} = 0$ because they become important only in the high-momentum region. The so calculated $I(p_x)$ is close to a parabola but with some small bulges originating from the region where the Bragg plane intersects the Fermi surface. This will be discussed in detail in section 3.

For the case (iii) U^* is not weak, many G vectors have to be included in the summation in equations (8) and (9). Among s,p-bonded materials the strongest U^* is expected for insulators. This will be discused elsewhere.

3. Results and discussion

We will now use Al to test the present new formalism to calculate the angular correlation distribution. Since a lot of work has been done for this material and good agreement has been obtained between the theoretical and experimental results [3–5, 11, 12, 30, 31], we will concentrate our attention on the fine structure, the anisotropic small bulge of the angular correlation distribution. The big isotropic bulge has been successfully explained using the many-body enhancement factor (see [3–5, 11, 12, 30, 31]) and we will not attempt to repeat this here. Our purpose is instead to test the PEP formalism and see whether or not it can give a good account of the experiments and also to compare it with the results of various conventional methods.

For Al metal we use only two parameters, U_{111} and U_{002}. A comparison between the Compton profile and ACAR of Al shows that the two curves are quite similar to each other. As argued above, this suggests that the electron pseudopotential parameters would be most reasonable as starting values for the potential parameters of PEP. Therefore, for U_{111} and U_{002}, we first choose the electronic parameters from [32], and thereafter

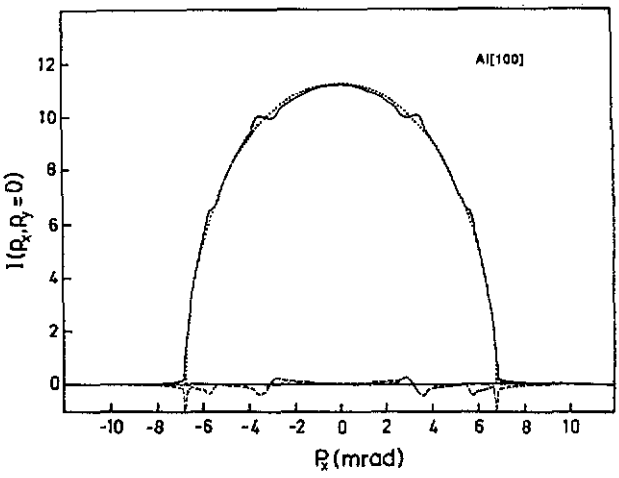

Figure 1. The two-dimensional angular correlation distribution along the Al[100] direction with $p_y = 0$. The full curve represents the calculated $I(p_x, p_y = 0)$, the dotted curve represents the circle $I_0(p_x, p_y = 0) = 2(E_F - p_x^2)^{1/2}$ with the potential $U^* = 0$ and the broken curve shows the difference $I(p_x, p_y = 0) - I_0(p_x, p_y = 0)$. The potential parameters are $U_{111} = 0.0179$ and $U_{002} = 0.0562$ Ryd.

we adjust them somewhat to give a better fit to the experimental results. We expect that the absolute values of the final parameters of PEP will be smaller than the electron pseudopotential parameters because, as discussed above, U^* is likely to be weaker than the corresponding electron pseudopotential due to the cancellation of the Coulomb potential.

In figure 1 we show the angular correlation $I(p_x, p_y = 0)$ along the [100] direction. In the calculations we find structures (bulges) around $p_x = 3$ and 6 mrad, which all are consistent with the experimental results [12]. The big isotropic bulge of the experimental curve $I_{ex}(p_x, p_y = 0)$ (a deviation from the circle $2(E_F - p_x^2)^{1/2}$ in the region of 2.5 mrad $< p_x <$ 6 mrad) in [12] has been explained by Berko *et al* [12, 30] based on the many-body momentum-dependent enhancement of Carbotte *et al* [7] and also by Chakraborty *et al* [3–5] based on the many-body energy-dependent enhancement. The experimental $I_{ex}(p_x, p_y = 0)$ can be divided approximately into three parts. The first part is the free potential part, i.e. a circle $2(E_F - p_x^2)^{1/2}$. The second part is a big isotropic bulge in the region of 2.5 mrad $< p_x <$ 6 mrad due to the effect of the electron–positron many-body enhancement. The third part is an anisotropic small bulge around $p_x = 3$ and one around 6 mrad. The second part is well understood through the work in [3–5, 12, 30], but is not present in our theoretical result because we have not included the many-body enhancement in our calculation. The reason is that, at this early stage of the PEP formalism, we will focus on the anisotropic small bulge, which is more directly related to the band-structure-like formalism itself rather than the many-body corrections. Therefore we will only consider the first and the third parts of the experimental results in the following discussion.

The calculated structure around $p_x = 3$ mrad is somewhat more pronounced than observed. This bulge is produced by the region where the Fermi surface intersects with the Bragg planes (002), (00−2), (111), (1−11), (11−1) and (1−1−1) both individually and mutually. Similarly the bulge around $p_x = 6$ mrad originates from the

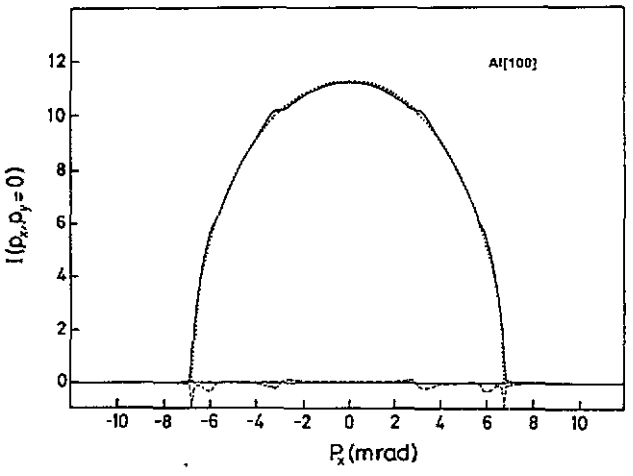

Figure 2. The two-dimensional angular correlation distribution along the Al[100] direction with $p_y = 0$. The notation is the same as in figure 1. The potential parameters are $U_{111} = 0.0170$ and $U_{002} = 0.03934$ Ryd.

region where the Fermi surface intersects with the Bragg planes (200), (111), (1 −11), (11 −1) and (1 −1 −1) both individually and mutually. It can be shown that the bulge produced by the Bragg plane perpendicular to the path of integration (which is the case for the bulge around $p_x = 3$ mrad) is larger than the bulge produced by the Bragg plane parallel to the path of integration (which is the case for the bulge around $p_x = 6$ mrad). The somewhat too strong effect found in the calculations can be understood by the fact that the Ashcroft pseudopotential parameters used in the calculation are stronger than the actual PEP potential parameters. Therefore we reduce the values of the parameters U_{111} and U_{002} to become 0.0170 and 0.03934 Ryd, instead of the initial values 0.0179 and 0.0562 Ryd, respectively. The so calculated $I(p_x, p_y = 0)$ is shown in figure 2. The bulges now become small, but there is still a minimum in the curve around $p_x = 3$ mrad, which is not seen in the experimental data [12]. There might be two reasons for this small difference. One is that the limited precision of the experiments might have smeared out the fine structure. The other is that the experiment was done at 100 K while both $I(p_x, p_y = 0)$ in figures 1 and 2 are calculated with $T = 0$ K. The temperature effect could be caused by several different mechanisms [4, 29]: (i) a temperature dependence of the effective mass of the positron; (ii) the Fermi–Dirac distribution of the electrons; (iii) the thermal expansion of the lattice constant a. This last effect of the lattice constant can be much reduced by presenting the ACAR as a function of the momentum p in units of $2\pi/a$ if the temperature change is small. It is more difficult, however, to include the correction for the positron effective mass in the calculation of ACAR. Usually this effect is estimated from the tail of the experimental ACAR, but we do not attempt to do it in this paper. The main effect of the Fermi–Dirac distribution is a smoothing of the ACAR curve, and this effect is hard to distinguish from the broadening due to instrumental resolution. The effect of the experimental resolution is usually taken into account by convoluting the theoretical curve with a proper experimental resolution function. In order clearly to display the small anisotropic bulge, we did not however apply such a convolution procedure.

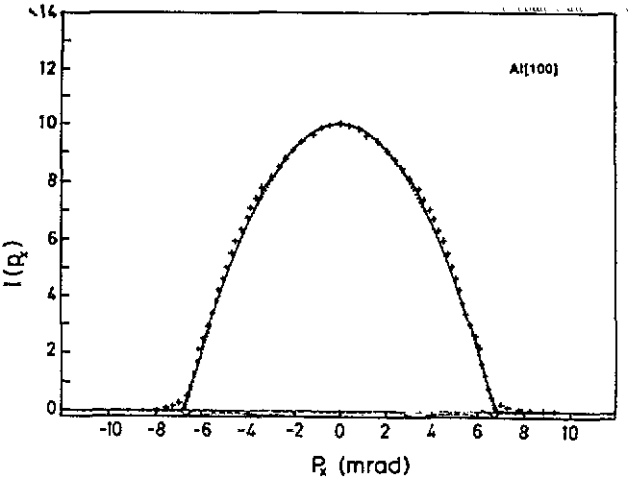

Figure 3. The one-dimensional angular correlation distribution (integrated over p_y) along the Al[100] direction. The full curve represents the calculated $I(p_x)$, the dotted curve represents the parabola $I_{\text{II}}(p_x)$ and the broken curve shows the difference $I(p_x) - I_0(p_x)$. The curve denoted by crosses represents the experiment of [31]. The potential parameters are the same as in figure 2, i.e. $U_{111} = 0.0170$ and $U_{(0)2} = 0.03934$ Ryd.

Figure 3 displays the calculated one-dimensional angular distribution $I(p_x)$ along the [100] direction with the new potential parameters. It agrees well with the experimental results of [11, 31], both as regards the shape and the small extended bulges around $p_x = 3.3$ and 6 mrad and also compares well with the theoretical result of [31] using a conventional APW (augmented plane wave) method. The difference between our theoretical calculation and the experimental curve [31], i.e. the large bulge from 3.3 to 5.6 mrad, can be accounted for by the effect of many-body enhancement, as was done in [31]. The computed $I(p_x)$ along the [111] direction with the same parameters is shown in figure 4. Again we reproduce the extended bulges around $p_x = 0$ and 6 mrad observed in the experiments [11], except that there is a small difference in the bulge around $p_x = 0$ mrad. Unlike the calculated distribution, the experiments show an asymmetric distribution around zero along the p_x direction. Possibly this slightly asymmetric result was due to the experimental conditions, which might have had a slightly different precision along different directions. Nevertheless the experimental results and the present calculations are remarkably consistent. For a further comparison the many-body enhancement should be included in the calculation and furthermore one needs experimental data of higher precision. Also systematic studies of the temperature effects should be undertaken.

We would also like to comment on the possible effects of the many-body interaction on ACAR. The many-body interaction can be treated in two ways. One is through the enhancement factor or de-enhancement factor. The other is through the wavefunction. It has been shown that the many-body effect in the Compton profile is isotropic and does not affect the anisotropy of the Compton profile [33]. Owing to the similarity between the many-body enhancement in the Compton profile and the positron–electron many-body energy-dependent enhancement in the angular correlation distribution, it is not unreasonable to expect that the many-body effects via the energy-dependent enhancement factor are more important for the large isotropic bulges (such as in the alkali metals

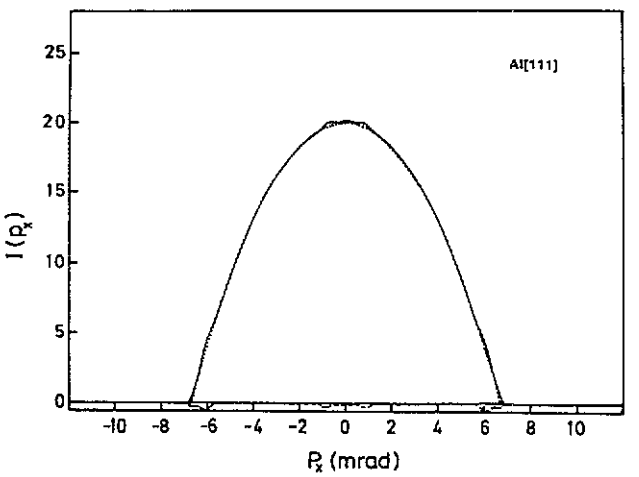

Figure 4. The one-dimensional angular correlation distribution (integrated over p_y) along the Al[111] direction. The full curve represents the calculated $I(p_x)$, the dotted curve represents the parabola $I_0(p_x)$ and the broken curve shows the difference $I(p_x) - I_0(p_x)$. The potential parameters are the same as in figures 2 and 3, i.e. $U_{111} = 0.0170$ and $U_{002} = 0.03934$ Ryd.

[7] and Al [3–5, 30]) than for the small and anisotropic bulges. Using the enhancement factor, one has successfully explained the bulges of ACAR curve in the alkali metals [7] and the large isotropic bulge in Al [3–5, 30]. This is consistent with the fact that the enhancement factor was obtained from the jellium model, which in itself is isotropic and in agreement with the conclusion of [30]. In contrast to the many-body effect via the energy-dependent enhancement factor, the many-body effect through the wavefunction together with the remaining potential is more directly responsible for the anisotropic bulges of ACAR. It is understood that two wavefunctions differing by one reciprocal lattice $\boldsymbol{G}$ will be strongly correlated. Thus the change of the total effective U_G due to the electron–positron interaction and many-body interaction is likely to have an appreciable effect on the wavefunction near the Bragg plane, especially when it coincides with the Fermi edge. As already discussed, the presence of the positron has no influence on the electron wavefunction for bulk ACAR calculations using the conventional formalism. Therefore the anisotropic bulge could sometimes not be well represented by the conventional method without using a model potential for the electron wavefunction calculation. However, in the simple metals these anisotropic bulges are sometimes too small to be resolved experimentally. Hence it is hard to draw a clear conclusion from the experiments on simple metals. In the semiconductor Si one can clearly notice these anisotropic many-body effects, something that will be discussed in a separate paper. In the metals Cr, Fe and Ce, it was found that the best agreement between the experimental and theoretical results is obtained by using a a parametrized model potential (instead of a self-consistent potential) for the electron wavefunction calculation together with a many-body enhancement correction [34, 35]. The mechanism behind this anomaly is not yet understood. If there is a change of the electron wavefunction induced by the positron, this would have an important effect on the angular correlation distribution, which might not be corrected by the many-body enhancement alone.

Within the present formalism the experimentally small anisotropic bulges are well reproduced. Some of the smallest bulges were not present in the results of [5], which might be due to a smoothing of both the experimental and theoretical curves. Because the theoretical as well as the experimental one-dimensional ACAR curve of Al are too close to the free-electron parabola, it was not attempted to analyse the isotropic effect of the many-body interaction. From the comparison between our calculated results and experiments, we do find that the positron–electron interaction and the many-body interaction have appreciable effects on the curves of ACAR in Al. The present PEP formalism does include these interactions in a phenomenological way in the calculation of ACAR.

4. Conclusions

In summary, we have shown that the present idea, i.e. directly solving the PEP equation, gives a new insight into the physics of positron–electron annihilation. In a qualitative analysis, it resolves some apparent paradoxes in the earlier treatments. In a quantitative calculation, it reproduces the extended bulges found experimentally and gives results consistent with the experimental findings. Clearly the present simple PEP formalism could be refined. It should be relatively easy to incorporate the many-body enhancement effect via the enhancement factor into this new formalism and it might be possible to develop a real-space PEP formalism. Before the PEP formalism is applied to a situation with a more localized positron, some problems need to be solved. One is the overall normalization of the wavefunction and another is the relationship between the potential parameters and their dependence on the crystal structure and temperature. This subject will be discussed elsewhere. We should emphasize that the PEP formalism at present is applied as a phenomenological scheme. Without experimental results and the experience obtained from calculations using the traditional formalism, it could not have been formulated. In the context of defects and materials with d and f electrons, the traditional formalism has of course a great advantage over the present PEP approach. Nevertheless it is reasonable to expect that the present PEP approach will be applicable to systems where the pseudopotential method is appropriate for the electron energy band calculation and will give results in agreement both with experiments as well as with the conventional formalism. Owing to the simplicity of the PEP formalism, It will be useful for understanding the general trends of the experimental ACAR. It might also play some role in the reconstruction of the three-dimensional ACAR from the two-dimensional ACAR. Further applications of the present PEP formalism are in progress.

Acknowledgments

One of the authors (LY) wishes to acknowledge stimulating discussions with Professor P Hautojärvi, LY and BJ would also like to acknowledge the Swedish Natural Science Research Council (NFR) for financial support.

References

[1] Berko S 1988 *Proc. 8th Int. Conf. on Positron Annihilation (Gent, Belgium)* unpublished

[2] Nieminen R M, Bornski E and Lantto L J 1985 *Phys. Rev.* B **32** 1377
[3] Chakraborty B, Siegel R W and Pickett W E 1981 *Phys. Rev.* B **24** 5445
[4] Fluss M J, Berko S, Chakraborty B, Haffmann K R, Lippel P and Siegel R W 1984 *J. Phys. F: Met. Phys.* **14** 2831
[5] Chakraborty B 1981 *Phys. Rev.* B **24** 7423; 1982 *Positron Annihilation* ed P G Coleman *et al* (Amsterdam) p 207
[6] West R N 1973 *Adv. Phys.* **22** 263
[7] Carbotte J P and Kahana S 1965 *Phys. Rev.* **139** A213
[8] Arponen J and Pajanne E 1979 *Ann. Phys., NY* **121** 343
[9] Arponen J and Pajanne E 1979 *J. Phys. C: Solid State Phys.* **12** L161
[10] Kontrym-Sznajd G and Sob M 1988 *J. Phys. F: Met. Phys.* **18** 1317
[11] Berko S and Plaskett J S 1958 *Phys. Rev.* **112** 1877
[12] Mader J, Berko S, Krakauer H and Bansil A 1976 *Phys. Rev. Lett.* **37** 1232
[13] Arponen J, Hautojärvi P, Nieminen R and Pajanne E 1973 *J. Phys. F: Met. Phys.* **3** 2092
[14] Jena P, Ponnambalam M J and Manninen M 1981 *Phys. Rev.* B **24** 2884
[15] Yongming Lou, Binglin Gu, Jialin Zhu, Chang Lee and Jiajiong Xiong 1988 *Phys. Rev.* B **38** 9490
[16] Yongming Lou 1988 *Proc. Int. Positron Workshop (München, 1988)* B17
[17] Lynn K G, Mills A P Jr, West R N, Berko S, Canter K F and Roelling L O 1985 *Phys. Rev. Lett.* **54** 1703
[18] Howell R H, Meyer P, Rosenberg I J and Fluss M J 1985 *Phys. Rev. Lett.* **54** 1698
[19] Jensen K O, Nieminen R M, Eldrup M, Singh B N and Evans J H 1989 *J. Phys.: Condens. Matter* **1** SA67
[20] In the two-component density-functional theory for the electron–positron system (see [2]), the Coulomb potentials for the electron and the positron are the same except for a difference in sign and both have contributions from all N electrons, all the ion cores and the positron. By definition, the self-interaction for the electron and the positron is removed by the corresponding exchange and correlation energy terms. However, in practice, the density-functional potential has to be approximated, and there is therefore an incomplete cancellation between the self-interaction and the exchange and correlation. The approximation gives rise to a small difference between the employed Coulomb potential for the electron and for the positron. We refer to the potential employed in the real calculation as the 'employed potential' while the 'true potential' is the potential that in principle is exact without any approximation in the density-functional theory.
[21] Stroud D and Ehrenreich H 1968 *Phys. Rev.* **171** 399
[22] Kubica P and Stott M J 1974 *J. Phys. F: Met. Phys.* **4** 1969
[23] Erskine J C and McGervey J D 1966 *Phys. Rev.* **151** 615
[24] Shiotani N, Sakai N, Ito M, Mao O, Itoh F, Kawata H, Amemiya Y and Ando M 1989 *J. Phys.: Condens. Matter* **1** SA27
[25] Brandt W and Reinheimer J 1971 *Phys. Lett.* A **35** 109
[26] Here we revise the Brandt–Reinheimer (see [13]) enhancement factor $\Gamma[n(r)]$ by substituting $2n(r)/n_0$ for the constant 2. This can be understood by the fact that the positron lifetime in vacuum is infinite. We will discuss it in more detail elsewhere
[27] Yongming Lou, Johansson B and Nieminen R M 1991 *Physica Scripta* at press
[28] West R N 1979 *Positrons in Solids* ed P Hautojärvi (Berlin: Springer) p 2
[29] Stott M J and West R N 1978 *J. Phys. F: Met. Phys.* **8** 635
[30] Berko S and Mader J 1975 *Appl. Phys.* **5** 287
[31] Okada T, Sekizawa H and Shiotani N 1976 *J. Phys. Soc. Japan* **41** 836
[32] Ashcroft N W 1963 *Phil. Mag.* **8** 2055
[33] Bauer G E W and Schneider J R 1984 *Phys. Rev. Lett.* **52** 2061
[34] Manuel A L, Singh A K, Jarlborg T, Genoud P, Hoffmann L and Peter M 1989 *Positron Annihilation* ed L Doriken-Vanpraet, M Dorikens and D Segers (Singapore: World Scientific) p 109
[35] Jarlborg T, Manuel A A, Peter M, Sanchez D, Singh A K, Stephan J-L, Walker E, Assmuss W and Hermann M 1989 *Poisitron Annihilation* ed L Doriken-Vanpraet, M Dorikens and D Segers (Singapore: World Scientific) p 266